

# Preparation of Ordered Mesoporous Alumina Particles via Simple Precipitation Method

Zainab Ramli <sup>1,\*</sup> and Rozaina Saleh <sup>2</sup>

<sup>1</sup> Ibnu Sina Institute for Fundamental Science Studies, Universiti Teknologi Malaysia, 81310 UTM Skudai, Johor, Malaysia

<sup>2</sup> Department of Chemistry, Faculty of Science, Universiti Teknologi Malaysia, 81310 UTM Skudai, Johor, Malaysia.

\* Author to whom correspondence should be addressed; E-mail: [zainab@kimia.fs.utm.my](mailto:zainab@kimia.fs.utm.my)

Received: 17 November 2008

## ABSTRACT

Several mesoporous alumina samples have been successfully prepared via simple and easy precipitation method by using inexpensive inorganic aluminium salts with ammonium acetate as precipitating agent. The aluminium acetate ( $\text{Al}(\text{CH}_3\text{COO})_3$ ) precipitate obtained was treated with nitric acid, acetone and ultrasonication to obtain mesoporous alumina. FESEM of the samples prepared from the treatment of nitric acid showed agglomeration of spherical nano-sized particle while TEM micrographs showed homogenous nano-sized pores in the range of 7-9 nm which agrees with data from nitrogen adsorption analysis.  $\text{Al}(\text{CH}_3\text{COO})_3$  treated with acetone followed by ultrasonic treatment exhibits narrower pore size distribution between 3.5-5.0 nm with higher surface area (198.36 m<sup>2</sup>/g) as compared to the sample without ultrasonic treatment. Acidity study of the alumina sample using pyridine adsorption indicates that the sample exhibits Lewis acidity.

| Mesoporous Alumina | Precipitation | Ultrasonication | Aluminium Acetate | Lewis Acidity |

## 1. Introduction

Mesoporous alumina with high specific surface areas and narrow pore size distributions was synthesized for the used in the fine chemical purification, catalysts, catalyst support and adsorbents [1]. Based on the value added property of the material, the unit price of mesoporous alumina has largely increases. For example, the mesoporous alumina absorbent for purifying liquid crystal (LC) is about 100 times higher than the unit price of alumina [2]. Conventional  $\gamma\text{-Al}_2\text{O}_3$ , composed of a mixture of macro, meso, and micropores in irregular sizes has been utilized. It is well known that micropores are easily plugged by undesirable cokes that are more or less formed during catalytic reactions, disturbs the diffusion of reactants and product. In addition, catalysts like existing  $\gamma\text{-Al}_2\text{O}_3$  which possesses wider pore-size distribution are prone to rapid deactivation [3]. Thus, it is highly desirable to synthesize porous alumina with high surface area and a narrow pore size distribution in a mesopore region as a catalyst and adsorbent to be utilized in numerous large-scale industrial processes.

Several methods have been used to synthesize the alumina particles. Preparation of mesoporous alumina by sol-gel technique from aluminium alkoxides in the presence of templates is well established [4,5]. However, aluminium alkoxides or boehmite powders raw materials were expensive. To decrease the cost of fabricating

mesoporous alumina, inexpensive inorganic salt raw materials have been used to replace aluminium alkoxide as aluminium precursor [6,7,8,9].

In this study, we attempt to prepare alumina by using inexpensive inorganic aluminium salts by easy precipitation method without the use of outside template. Instead, the aluminium acetate ( $\text{Al}(\text{CH}_3\text{COO})_3$ ) which obtained from the precipitation of various aluminium salts with acetate ion ( $\text{CH}_3\text{COO}^-$ ) will be the precursor for the formation of mesoporous alumina. In this case, the acetate ion is acting as an organic template which will contribute to the formation of pores to the synthesized alumina after calcination process.

## 2. Materials and Methods

### 2.1. Synthesis of Alumina with Nitric Acid Treatment

$\text{Al}(\text{NO}_3)_3 \cdot 9\text{H}_2\text{O}$  (0.05 mol) or 0.025 mol of  $\text{Al}(\text{SO}_4)_3 \cdot 16\text{H}_2\text{O}$  were prepared in 50 mL distilled water and  $\text{NH}_4(\text{CH}_3\text{COO})$  (11.56 g) was added to the solution under vigorous stirring to obtain an optically transparent and colourless solution. After 24 hours, an amount of  $[\text{H}^+]/[\text{Al}^{3+}] = 0.05$  mol ratio of nitric acid (69-70%, JT Baker) was added to the precipitate formed. The mixture was stirred 24 hours at various temperatures. Aging process was carried out at 75°C for 24 hours. Finally, the supernatant was removed from the precipitate by centrifugation. The precipitate was washed by distilled water for several times. Then the sample was dried in an oven at 100°C for 24 hours. All samples were denoted in Table 1:

**Table 1:** Notation of samples prepared with the treatment of nitric acid

Notation	Nitric Acid Treatment (°C)
A-AS-70	70
A-AS-RT	Room Temperature
A-AN-70	70
A-AN-RT	Room Temperature

### 2.2. Synthesis of Alumina with Acetone Treatment

The same procedure as described above was carried out. 100 mL of acetone was added to cause precipitation of the aluminium acetate particles under vigorous stirring for 24 hours. The precipitate and the solution were decanted after centrifugation at 3000 rpm. Then the sample was dried in an oven at 100°C for 24 hours. The obtained white powder was calcined at 750°C for 10 hours in air atmosphere. The sample was denoted as B-DW.

### 2.3. Ultrasonic Treatment

Sample prepared from nitric acid treatment at room temperature and sample prepared with the treatment of acetone were treated with ultrasonic treatment using JAC ultrasonic Cleaner (Lab Companion 1505, 370 Watt) at high strength. The samples from nitric acid treatment and from the treatment of acetone were denoted as A-AN-S30 and B-S30-DW respectively.

## 2.4. Characterization of the Catalysts

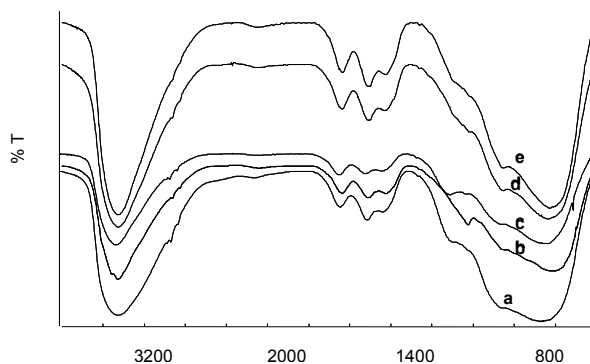
Infrared spectra of the samples were obtained on Perkin Elmer (1600 series) spectrometer using the KBr wafer technique. The spectra were recorded at room temperature with  $4\text{ cm}^{-1}$  resolution between  $1400\text{ cm}^{-1}$  -  $400\text{ cm}^{-1}$ . For the analysis using FESEM, the samples were coated with gold/titanium on respective sputter. The samples were scanned using JEOL JSM-6330F fields emission scanning electron microscope operating at 15 kV. For TEM analysis, the sample was prepared on 300 mesh copper grid and scanned using JEOL JEM2100 Transmittance Electron Microscope operating at 200 kV. The nitrogen adsorption-desorption measurements of calcined samples were performed using Micromeritics ASAP 2010 volumetric adsorption analyzer. The XRD pattern of all samples were recorded on Bruker Advance D8 using Siemens 5000 diffractometer with  $\text{Cu K}\alpha$  radiation ( $\lambda = 1.5418\text{ \AA}$ ,  $\text{kV} = 40$ ,  $\text{mA} = 40$ ). The powder sample was firstly spread equally on the sample holder to form a thin and smooth layer. The sample was scanned in the  $2\theta$  scale of  $1.5^\circ$  to  $80^\circ$  with step size  $0.05^\circ$  per second.

For the acidity measurement, the sample was ground to a fine powder and pressed into very thin self-supporting wafer containing  $10\text{ mg cm}^{-2}$  samples. The sample disc was mounted in an IR cell equipped with  $\text{CaF}_2$  windows and evacuated at  $400^\circ\text{C}$  for overnight and under  $10^{-4}$  mbar pressure. After pre-treatment, the sample was cooled to room temperature and the IR spectrum was recorded. The above sample was then exposed to 10 torr of pyridine at room temperature for 10 minutes. Desorption of pyridine was carried out by evacuating step by step for 1 hour at  $100\text{--}400^\circ\text{C}$ . The infrared spectra were recorded using Perkin Elmer 1600 Spectrometer with a resolution of  $2\text{ cm}^{-1}$ . The integrated intensities of the desired bands were determined and used as a measure of the amounts of Brønsted-bound pyridine (B-py) and Lewis bound pyridine (L-py), respectively.

## 3. Results and Discussion

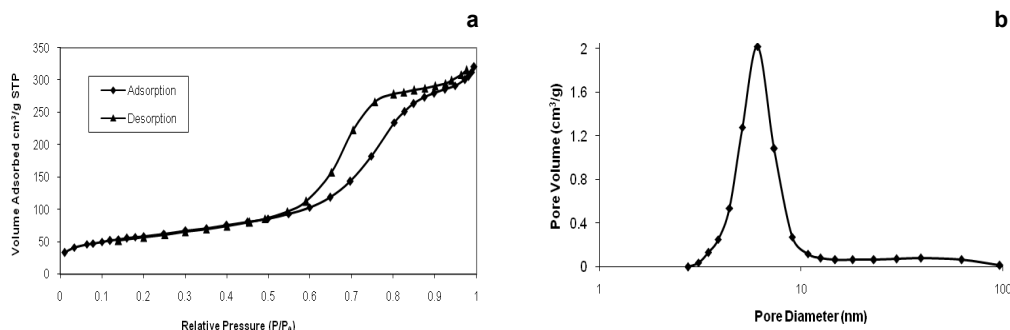
### 3.1. Synthesized Alumina with Nitric Acid Treatment

Figure 1 shows the IR spectra for the synthesized alumina. All spectrums are equally the same and show no obvious differences between each other. The broad band at  $3200 - 3700\text{ cm}^{-1}$  is assigned to the stretching vibration of the  $-\text{OH}$  group bonded to Al cation and peak at  $1638\text{ cm}^{-1}$  corresponds to water of hydration. The shoulder band at  $1410\text{ cm}^{-1}$  corresponds to  $-\text{NO}_3$  group from  $\text{HNO}_3$  added for acid treatment while peak at  $738\text{ cm}^{-1}$  is assigned to the bending vibrations of Al-O. The pattern of this bending band is an indication of alumina with gamma phase [10].



**Figure 1:** Infrared spectra of a) A-AS-RT b) A-AN-70 c) A-AN-S30 d) A-AN-RT e) A-AS-70-S20

Nitrogen adsorption and desorption were measured to investigate the pore diameter, pore volume and pore size distributions of the alumina sample after being treated with ultrasonication. Figure 2(a-b) shows the isotherm and pore size distribution of sample A-AN-S30. As shown in Figure 2a, the sample exhibits type IV isotherm which is the characteristic of mesoporous material. The isotherm also showed two steps in the hysteresis loop indicating the presence of a small amount of large mesopores in the sample that can be seen in the pore size distribution curves in Figure 2b. According to IUPAC classification, the sample exhibits a mixture of cylinder type (H1) and stacked plane type (H3) of pores. Pore size distributions curve was shown in Figure 2b.



**Figure 2:** (a) BJH pore-size distributions and (b) N<sub>2</sub> adsorption-desorption isotherms of sample A-AN-S30.

This A-AN-S30 sample exhibits a narrow pore size distribution with FWHM peak is 2.7 nm and centered at 6 nm. This sample also exhibits higher BET surface area (212 m<sup>2</sup>/g) as compare to commercial  $\gamma$ -alumina (BET surface area  $\sim$  90-100 m<sup>2</sup>/g). and high pore volume with average pore diameter 8.8 nm

All the FESEM micrographs of the synthesized alumina were shown in Figure 3(a-e). In general all samples produced spherical nano-sized particles with strong agglomeration. A similar phenomenon was also reported by H.S. Potdar *et al* [7]. There is no significant effect of temperature as well the ultrasonic treatment on the surface morphologies of the synthesized alumina. It suggests that, the energy heat and the ultrasonic were unable to disperse the particles.

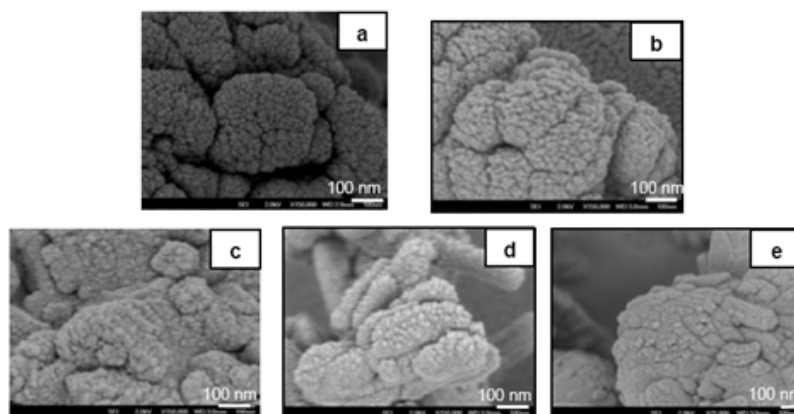


**Figure 3:** FESEM micrographs of the synthesized alumina. (a) A-AS-RT (b) A-AS-70 (c) A-AN-RT (d) A-AN-70 (e) A-AN-S30

Transmission electron microscopy was used to evaluate the surface morphology of the A-AN-RT. As shown in Figure 4(a), the alumina treated with nitric acid at room temperature (A-AN-S30) consists of wormhole [11] or sponge-like in meso-range pore, indicating the advantage of a highly inter-connected pore system[12]. This result is in agreement with the data from the  $N_2$  adsorption analysis. Figure 4(b) depicts the high magnification TEM micrograph of the same sample (A-AN-RT). It is clearly shown that this mesoporous material exhibits a regular worm-like channel motif, however, without clear indication of the long-range channel packing order. Similar TEM pictures were also reported by the other author [5], who claimed that the packing of the channel system is more or less random, in spite of the presence of one X-ray diffraction line.

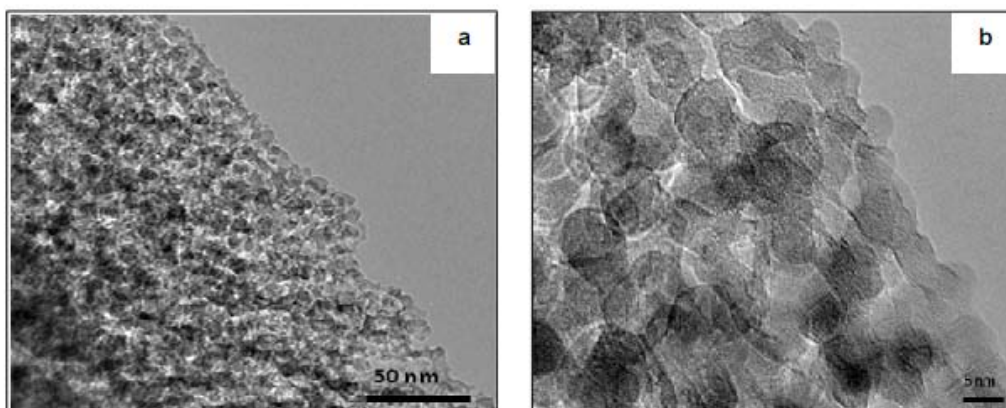


**Figure 4:** TEM micrographs of the A-AN-S30 (a) low magnification factor (b) high magnification factor

### 3.2. Synthesized Alumina with Acetone Treatment

Figure 5 shows the infrared spectra of the synthesized alumina after calcination at 700°C. The IR pattern obtained for these samples are similar to that of alumina samples prepared by nitric acid treatment indicating that alumina having  $\gamma$ -phase structure. The important vibration bands and their wave number are summarized in Table 2.

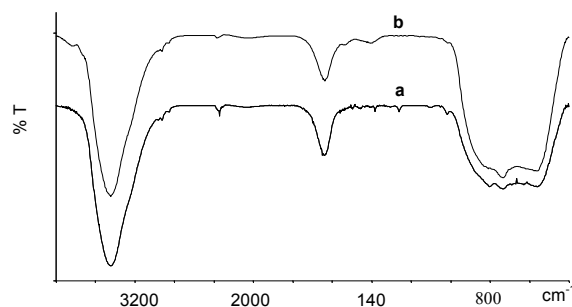


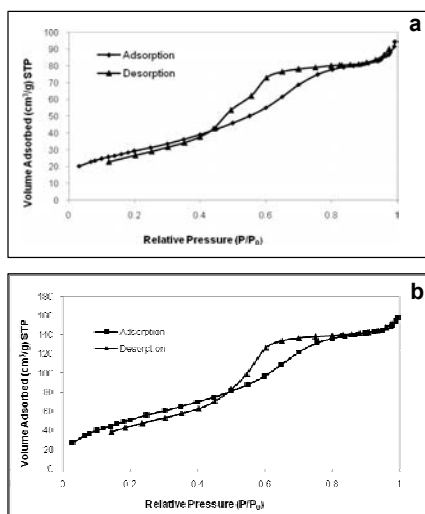
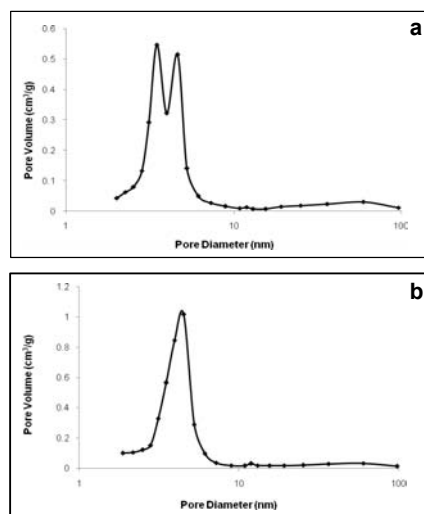
**Figure 5:** Infrared spectra of samples a) B-S30-DW b) B-DW

**Table 2:** Assignments of FTIR bands of B-S30-DW and B-DW

Characteristic Bands	Wavenumber / $\text{cm}^{-1}$
–OH (stretching)	3450
Water of hydration	1636
Al-O (bending)	738
Al-O-Al (vibration)	620

Figure 6 and Figure 7 present the  $\text{N}_2$  adsorption isotherm and BJH pore size distributions for sample B-DW (without ultrasonic treatment) and B-S30-DW (with ultrasonic treatment) respectively. From Figure 6, both samples also present type IV isotherm as the sample treated with nitric acid, which is characteristic of mesoporous material. The appearance of type H2 hysteresis loop indicates the presence of “cylindrical” type pores in both synthesized alumina. However, from the isotherm of sample B-DW (Figure 6a), two shoulders were observed at the desorption isotherm. This might due to the presence of non uniform cylindrical pores. It was further proved by BJH pore size distribution in Figure 7a, showing a dual peaks suggesting that 2 types of ordered mesopores exist in the sample. The pores were introduced by framework mesopore and textural pore of the alumina [13]

Action of ultrasonic energy on the sample alumina sample has successfully homogenized the pore size distribution. Sample B-S30-DW in Figure 7b shows a single peak with very narrow pore size distribution with 1.5 nm FWHM and centered at 4.3 nm. On the other hand, sample B-DW shows pore size distribution between 3.0 - 5.0 nm with dual peaks centered at 3.5 and 4.5 nm. Isotherms also.

**Figure 6:**  $\text{N}_2$  adsorption-desorption isotherm plots of a) B-DW and b) B-S30-DW**Figure 7:** BJH pore size distribution of a) B-DW and b) B-S30-DW

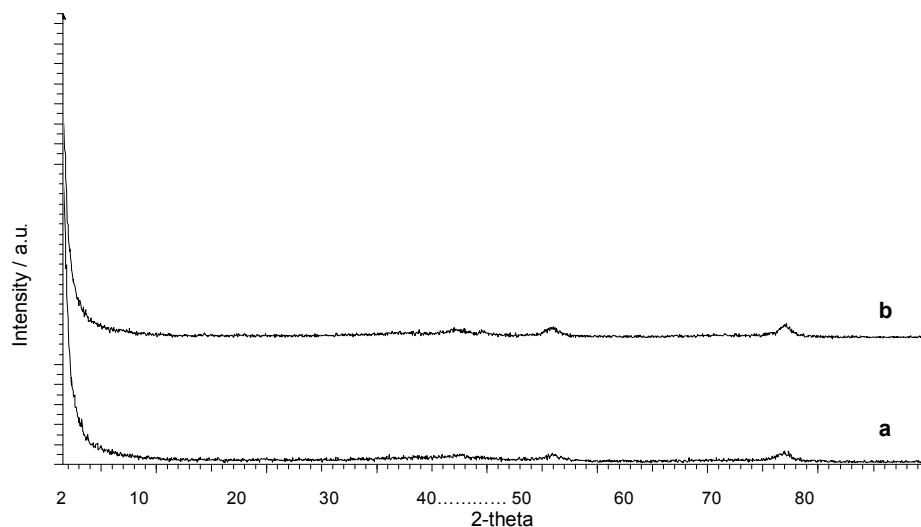
show a small increase in volume adsorbed at relative pressure approaching 1. It indicates that samples contain only small amount of pores resulting from interparticles aggregation. The narrow pore distribution obtained for the samples might be contributed by the acetate anion of the aluminium acetate which in this case acts as pore directing agents

Table 3 shows the BET surface area, total pore volume and average pore diameter of the synthesized alumina with acetone treatment. For the ultrasonic treated synthesized alumina (B-S30-DW), the surface area, pore volume and average pore diameter is higher compare to sample without the treatment of ultrasonic. Thus, the ultrasonic treatment did affect the surface area and porosity of the prepared samples. The energy from the ultrasonication applied on sample B-S30-DW, can caused particles to disintegrate to smaller particles and successfully distribute the particles. The smaller particles lead to high surface area alumina.

**Table 3:** The surface area and porosity of the samples prepared without ultrasonic treatment (B-DW) and with ultrasonic treatment (B-S30-DW),

Sample Notation	Surface area (BET) (m <sup>2</sup> /g)	Total pore volume (cm <sup>3</sup> /g)	Average pore diameter (nm)
B-DW	102.17	0.15	5.49
B-S30-DW	198.36	0.25	4.90

The XRD patterns of samples B-DW and B-S30-DW are illustrated in Figure 8. Both samples show the XRD powder patterns of  $\gamma$ -alumina with increased intensity when approaching low angle ( $2\theta < 3^\circ$ ). When examined closely sample B-S30-DW showed higher intensity at low angle compared to sample B-DW. This is an indication that the synthesized alumina treated with ultrasonication may have a well organized pore distribution [12]. This was proven by the result from BJH pore size distribution in Figure 7b.



**Figure 8:** XRD pattern of samples a) B-S30-DW and b) B-DW

### 3.3. Acidity Study

Acidity study of sample B-S30-DW was carried out. Spectra of pyridine adsorbed on acid sites are shown in Figure 9. The peaks appear at 1612 and 1452  $\text{cm}^{-1}$  correspond to Lewis acid bound pyridine (L-py). The band at 1492  $\text{cm}^{-1}$  can be assigned to pyridine associated with both Brönsted and Lewis sites (LB-py). The peaks at 1578 and 1595  $\text{cm}^{-1}$  were assigned to physisorbed and hydrogen bonded pyridine respectively. These two peaks diminished upon desorption at 200 °C. The summary of the pyridine adsorption wavenumbers and their assigned bonding were summarized in Table 4.

It can be seen that the intensity of the L-py peak decreased with the increasing of temperature, but shifted to higher wavelength, suggesting that sample B-S30-DW possess strong Lewis acid site. The formation of Lewis acid sites on alumina is simplified in Figure 10. When alumina is heated at more than 200°C, the surface hydroxyl group will be eliminated from the surface and created Lewis acid and Lewis base sites. When pyridine is introduced to the surface of alumina, the pyridine molecule will attach at the Lewis acid site since pyridine is a base molecule.

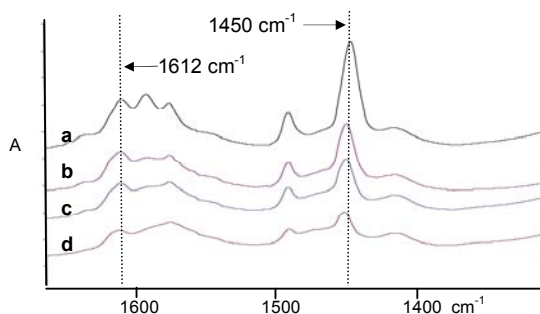


**Figure 9:** FTIR spectra of adsorbed pyridine on B-S30-DW sample, obtained after pyridine desorption at a) 100°C b) 200°C c) 300°C d) 400°C

**Table 4:** Integrated area at respective desorption temperature of sample B-S30-DW

Desorption Temperature (°C)	Pyridine Region ( $\text{A}/\text{cm}^{-1}$ )
100	2.1197
200	1.1080
300	0.7502
400	0.3709

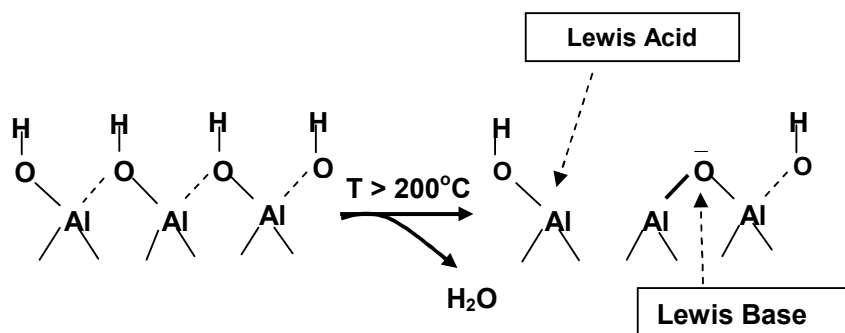


**Figure 10:** The formation of Lewis acid and base site on the surface



#### 4. Conclusion

Narrow pore size distributions alumina has been successfully synthesized via simple and easy precipitation method using ammonium acetate as precipitating and pore directing agent. Alumina prepared by both nitric acid and acetone treatment followed by ultrasonication produce highly organized pore size distributions in mesopore region as proved by nitrogen adsorption and TEM analysis. All samples show  $\gamma$ -alumina phase from FTIR spectra and proven by XRD diffractograms. Acidity study indicates that alumina sample possesses Lewis acid site. Since there are no significant difference in the pore distribution and BET surface area of the alumina obtained by both acid and acetone treatments, highly organized pore distribution and high surface area alumina are best prepared by acetone treatment followed by ultrasonication since this preparation involved is easier method and time saving.

#### 5. Acknowledgements

The authors acknowledge the Ministry of Higher Education (MOHE) for the Financial Support under FRGS (vot. no. 78076) and Ministry of Science, Technology and Innovation (MOSTI) for National Science Fellowship.

#### 6. References

- [1] Q. Liu, A. Wang, X. Wang, and T. Zhang, *Micropor. Mesopor. Mater.* 100 (2007) 35.
- [2] T. B. Du, S. M. Jang and B. W.B. Chen, *Chem. Eng. Sci.* 62 (2007) 4864.
- [3] T. Seki, S. Ikeda and M. Onaka, *Micropor. Mesopor. Mater.* 96 (2006) 121.
- [4] N. Yao, G. Xiong, Y. Zhang, M. He and W. Yang, *Catal. Tod.* 68 (2001) 97.
- [5] J. Čejka, *Appl. Catal. A* 254 (2003): 327.
- [6] J. Y. Park, S. G. Oh, U. Paik and S. K. Moon, *Mater. Lett.* 56 (2002) 429.
- [7] H. S. Potdar, K. W. Jun, J. W. Bae, S. M. Kim and Y. J. Lee, *Appl. Catal. A.* 321 (2007) 109.
- [8] S. Wang, X. Li, S. Wang, Y. Li, and Y. Zhai, *Mater. Lett.* 2008. (Article in Press).
- [9] Y. Zhang, X. Shi, J.M. Kim, Y. Sun, and S. Peng, *Catal. Tod.* 93 (2004) 615.
- [10] C. H. Seek and J. K. L. Lai, *Nano Struct. Mater.* 8 (1997) 605.
- [11] N. Zilkova, A. Zukal and J. Čejka, *Micropor. Mesopor. Mater.* 95 (2006) 176.
- [12] Y. Kim, C. Kim, P. Kim and J. Yi, *J. Non. Cryst. Sol.* 351 (2005) 550.
- [13] C. N. Satterfield, *Heterogenous Catalysis in Practice*. United States of America: Mc Graw Hill. 1980.